

ATTITUDE CONTROL MECHANIZATION TO DE-ORBIT SATELLITES USING SOLAR SAILS

Ozan Tekinalp,^{*} Omer Atas[†]

Utilization of solar sails for the de-orbiting of satellites is investigated. The proper attitude maneuver mechanization is proposed to harvest highest solar drag for Earth orbiting satellites. The maneuver is realized using a to-go quaternion calculated from body fixed frame measurements. The success of the attitude control during the continuous, as well as abrupt maneuvers is shown through simulations. The reduction in semi major axis due to the solar drag is shown to be similar in orbits with different inclinations.

INTRODUCTION

The possibility of collision of the artificial satellites with the Earth orbiting object is rapidly increasing. It is estimated that there is about 5.500 tons of debris in Earth orbit due to abandoned satellites, upper stages of launch vehicles, etc. In addition, the number of objects is estimated to grow at a rate of 5% every year¹. United States Space Command is tracking thousands of debris larger than 10cm in diameter². In particular, the Low Earth Orbit altitudes are especially crowded, and the risk of collision is rapidly increasing. The new procedures set forth by NASA requires the spacecraft in low Earth orbit, shall remain in region no more than 25 years after the end of mission³. A similar regulation is about to put into force in the European Union as well⁴. Normally, sufficient amount of fuel with working thrusters are necessary to de-orbit a satellite, just as the thrusters are needed for placing them to their orbit. However, this requires carrying a large amount of additional de-orbiting fuel with the satellite.

Utilization of solar sails for de-orbiting satellites is a new concept,. The idea is to carry a light weight solar sail to orbit, and deploy it at the end of life for the purposes of de-orbiting the satellite. The Aerospace Engineering Department of METU is involved in an FP7 collaborative project to design, build and launch a CubeSat to demonstrate the utilization of solar sails for de-orbiting satellites (European Union FP7 project, Project no: 263248, 2010). The concept utilization of solar sails has been theoretically investigated for rising satellite orbits, as well as for interplanetary travel⁵. The solar sail technology for interplanetary travel was also successfully shown in 2010 on Ikarus satellite. The sail types to be used, as well sail folding and deployment mechanisms has been thoroughly investigated in the literature. However, it is not sufficient to deploy

^{*} Professor, Middle East Technical University, 06800, Ankara, Turkey

[†] Graduate Research Assistant, Professor, Middle East Technical University, 06800, Ankara, Turkey.

the sail once in orbit, but to properly orient the sail with respect to the sun direction to get sufficient solar drag from the sun for de-orbiting. Thus, an attitude control has to be active to continuously orient the sail. This paper addresses the attitude control of satellites with de-orbiting solar sails.

In the following section, the equations for solar sail and optimal steering are given. It is followed by the attitude control equations. The simulation results are presented and discussed next. Finally, conclusions are given.

FORMULATION OF THE PROBLEM

The momentum carried by the electrical waves is transferred to an object when it hits an absorbing or a reflecting surface. According to Maxwell's electromagnetic equations the magnitude of the radiation pressure on an absorbing surface may be given as:

$$P = \frac{W}{c} \quad (1)$$

where, P is radiation pressure, W radiation flux and c is the speed of light. For a reflecting surface the magnitude of the radiation pressure is doubled. The direction of radiation force on a perfectly reflecting solar sail is in the normal direction of sail ⁵.

On a perfectly reflecting solar sail the incident light is reflected completely. As shown Figure 1, incidence angle is equal to reflection angle with respect to sail normal. Since the incidence and reflection angles are equal, the tangential components of the solar radiation pressure due to the incidence and reflection radiation cancel each other. Then the resultant force is in the direction of sail normal.

$$\mathbf{F} = 2PA(\mathbf{u}_i \cdot \mathbf{n})^2 \mathbf{n} \quad (2)$$

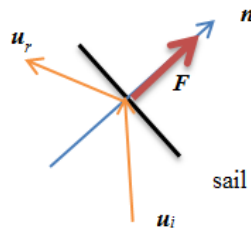


Figure 1 Solar radiation force

For orbital decay the radiation force vector must be oriented in such a way to decrease the orbital energy. For this reason the sail must be oriented such that the component of the drag due to solar radiation is maximized. Consider the orbital equation given in with gravitational attraction, and solar sail characteristic acceleration ⁵:

$$\frac{d^2 \mathbf{r}}{dt^2} + \mu \frac{\mathbf{r}}{r^3} = K(\mathbf{s} \cdot \mathbf{n})^2 \mathbf{n} \quad (3)$$

K is specific acceleration of solar sail due to solar force, μ earth's gravitational parameter, and \mathbf{n} is sail normal, and \mathbf{s} sun-line direction vector. An energy equation may be obtained by multiplying equation (3) by velocity vector, \mathbf{v} .

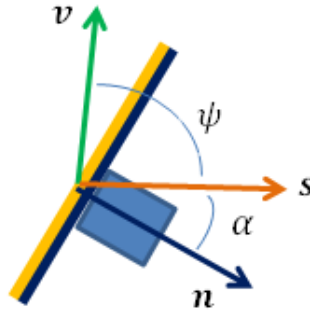


Figure 2 Solar sail for maximum drag

$$\frac{d^2\mathbf{r}}{dt^2} \cdot \mathbf{v} + \mu \frac{\mathbf{r} \cdot \mathbf{v}}{r^3} = K(\mathbf{s} \cdot \mathbf{n})^2 \mathbf{n} \cdot \mathbf{v} \quad (4)$$

Since the left hand side of the above equation represents the rate of change of total energy⁵

$$\frac{dE}{dt} = K(\mathbf{s} \cdot \mathbf{n})^2 \mathbf{n} \cdot \mathbf{v} \quad (5)$$

The right hand side of the equation may be written as:

$$(\mathbf{s} \cdot \mathbf{n})^2 \mathbf{n} \cdot \mathbf{v} = \cos^2 \alpha \cos(\psi + \alpha) \quad (6)$$

Where ψ is the angle between sunline and the velocity vector and α is the angle between sunline and the solar sail normal as shown in Figure 2. The angle that will result on maximum solar drag, or solar thrust, may be found from⁵,

$$\frac{d}{d\alpha} [\cos^2 \alpha \cos(\psi + \alpha)] = 0 \quad (7)$$

Solving the above equation gives the locally optimal angle is calculated as

$$\alpha = \frac{1}{2} \left[\pi - \psi - \sin^{-1} \left(\frac{\sin \psi}{3} \right) \right] \quad (8)$$

From Figure 3 solar sail orientation may be observed. Starting from point '0', the sail reflective side is up. In other words, the sail normal is perpendicular to the sail, but directed out from the non-reflecting side of the sail. Thus, according to the locally optimal steering law, the sail, together with the satellite, rotates 180° in one period. At the end of the period, this time sail bright surface is looking down. Then, the satellite must be flipped over by 180° to bring it to the initial shiny side up orientation. Consequently, for optimal steering, after almost a smooth rotation of

the satellite, a very rapid flip over is needed. This should be carefully planned not the saturate attitude control actuators.

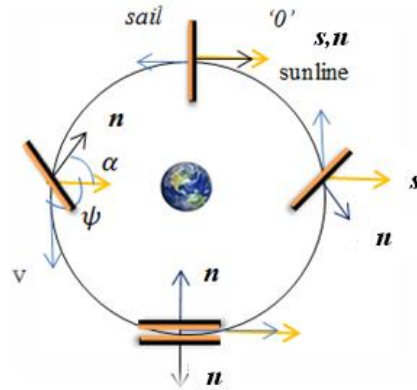


Figure 3 Locally optimal steering law for an Earth orbit in the ecliptic plane

The locally optimal angular orientation of solar sail normal with respect to sunline may be obtained as a function of the angle between velocity vector and sunline direction. Then it is necessary to develop an algorithm to find the desired attitude for highest solar drag to be used in de-orbiting. First assume that the satellite x -axis is in the normal direction of the solar sail (Fig. 2). Thus, the solar sail direction is originally $\mathbf{n} = \mathbf{i}$. Both the direction of the sun and the direction of the velocity vector are measured in the body fixed frame. Then the axis to be rotated around to harvest the proper solar force will be perpendicular to the plane formed by these two vectors:

$$\boldsymbol{\lambda} = \frac{\mathbf{s} \times \mathbf{v}}{\|\mathbf{s} \times \mathbf{v}\|} \quad (9)$$

Then a quaternion to rotate \mathbf{s} by α around the axis $\boldsymbol{\lambda}$ is:

$$q = \left[\boldsymbol{\lambda} \sin\left(\frac{\alpha}{2}\right) + \cos\left(\frac{\alpha}{2}\right) \right] \quad (10)$$

Then the desired sail normal direction may be calculated using quaternion rotations as:

$$\mathbf{n}_d = q\mathbf{s}q^* \quad (11)$$

Once the desired normal direction is found, the to-go quaternion to carry out the attitude control may be found from current sail normal direction and desired sail normal direction. Since two vectors are known the angle between them may be found from,

$$\beta = \cos^{-1} \left(\frac{\mathbf{n} \cdot \mathbf{n}_d}{\|\mathbf{n}\| \|\mathbf{n}_d\|} \right) \quad (12)$$

The direction of the *to-go quaternion* may be found from

$$\mathbf{e} = \frac{\mathbf{n} \times \mathbf{n}_d}{\|\mathbf{n} \times \mathbf{n}_d\|} \quad (13)$$

$$\mathbf{t} = \left[\mathbf{e} \sin\left(\frac{\beta}{2}\right) + \cos\left(\frac{\beta}{2}\right) \right] \quad (14)$$

This to-go quaternion is the conjugate of the more popular error quaternion⁶. Given the to-go quaternion, nonlinear attitude control of the spacecraft may be carried out using a the following positive definite Lyapunov function⁶:

$$\mathbf{V} = \boldsymbol{\omega}^T \mathbf{K} \mathbf{J} \boldsymbol{\omega} + 2(1 + t_4) \quad (15)$$

Where \mathbf{J} is the inertia matrix, $\boldsymbol{\omega}$ is angular velocity vector. For stability, the time rate change of this function must be negative definite.

$$\dot{\mathbf{V}} = \boldsymbol{\omega}^T \mathbf{K} \mathbf{J} \dot{\boldsymbol{\omega}} + 2\dot{t}_4 \leq -\boldsymbol{\omega}^T \mathbf{C} \boldsymbol{\omega} \quad (16)$$

Substituting,

$$\dot{\boldsymbol{\omega}} = \mathbf{J}^{-1}(-\tilde{\boldsymbol{\omega}} \mathbf{J} \boldsymbol{\omega} + \mathbf{u}) \quad (17)$$

Where, $\tilde{\boldsymbol{\omega}}$ is the matrix to carry out vector multiplication with $\boldsymbol{\omega}$, and remembering that,

$$\dot{t}_4 = \frac{1}{2} \boldsymbol{\omega}^T \mathbf{t} \quad (18)$$

The control torque that will carry out the slew maneuver is obtained as:

$$\mathbf{u} = \tilde{\boldsymbol{\omega}} \mathbf{J} \boldsymbol{\omega} + \mathbf{K} \mathbf{t} - \mathbf{C} \boldsymbol{\omega} \quad (19)$$

Normally, for a given a desired attitude with respect to an inertial frame and the current attitude of the spacecraft, the to go quaternion is calculated using proper quaternion multiplication. However, in the above mechanization, the to-go quaternion is calculated directly from current sail normal direction and desired sail normal direction in the body frame as presented above.

Where, \mathbf{t} is the vector part of the to-go quaternion vector and \mathbf{K} and \mathbf{C} , are the controller gains. These gains may be tuned based on the desired damping ratio and natural frequency as follows⁶:

$$\begin{aligned} \mathbf{K} &= 2\omega_n^2 \mathbf{J} \\ \mathbf{C} &= 2\xi\omega_n \mathbf{J} \end{aligned} \quad (20)$$

The equation of the orbital motion of a satellite is represented with respect to the Earth centered inertial coordinate system as shown in Figure 4. Thus, the X axis is towards the Vernal equinox direction, and XY lies in the equatorial plane forming an orthogonal right handed coordinate system. Since the date is chosen as 22nd of September, Y-axis is along the line formed by the cross section of the orbital and ecliptic plane.

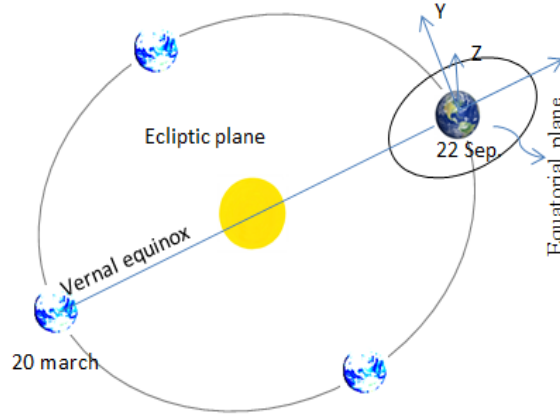


Figure 4 Orientation of Earth centered inertial coordinate system.

Then the equations of the satellite orbital motion, neglecting the higher order harmonics of the gravitational attraction, may be expressed in the inertial frame as:

$$\begin{aligned}\ddot{X} &= -\mu \frac{X}{r^3} + f_x \\ \ddot{Y} &= -\mu \frac{Y}{r^3} + f_y \\ \ddot{Z} &= -\mu \frac{Z}{r^3} + f_z\end{aligned}\tag{21}$$

where, $r = \sqrt{X^2 + Y^2 + Z^2}$, and f_x, f_y, f_z are the components of the solar radiation force acting on the spacecraft.

RESULTS AND DISCUSSION

A simulation code is developed to simulate the satellite orbital motion as well as attitude dynamics. Since the purpose of this work is to show the orbital decay, and the associated attitude control problem, only a simple gravitational field without the spherical harmonics, is considered in the simulation, as defined in Equation (21). The physical properties of the satellite are listed in Table 1 together with the controller parameters. A non-diagonal matrix is chosen to include the inertial coupling between the coordinates. The control system parameters on the other hand are chosen for the system to have good damping and acceptable response time.

Table 1. Properties of the satellite

Parameter	Value
Mass	6 [kg]
Inertia	[7.1589 -0.03 -0.03;-0.03 3.5794 -0.03;-0.03 -0.03 3.5794] [kgm ²]
Solar sail area	25 [m ²]
Natural Frequency	$\omega_n=0.01$ [rad/s]
Damping Ratio	$\xi = 0.7$

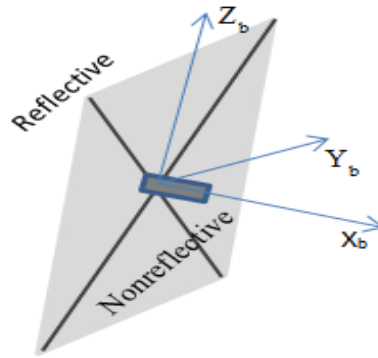


Figure 5 Body fixed coordinate system

The simulation results are presented in figures 7-18. In all the cases, the satellites are initially assumed to be in a circular orbit with 42000km semi major axis. In addition, the satellite body axis is initially at the desired orientation. Three cases are considered. In Case I, the initial orbit is an equatorial one. In the remaining two cases, orbits with 45 and 90 degree inclinations are considered. For these orbits, the right ascension of ascending nodes are taken as 90 degrees.

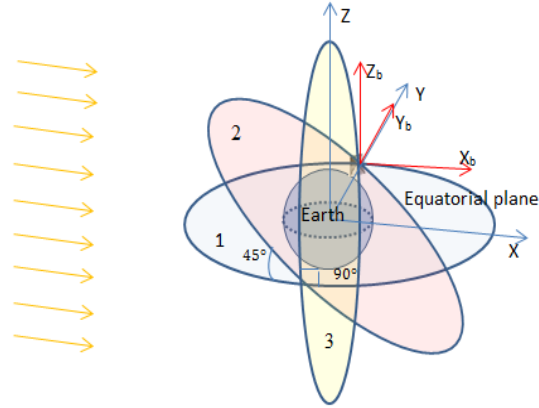


Figure 6 Three initial Orbit and initial solar sail position

In Figure 7 the spacecraft attitude history is given. It may be observed from the figure that the pitch and yaw angles do not change at all. However, yaw angle changes continuously from -90 to 90 degrees. There is also a flip along y-axis is observed at periodic orbit locations, since only one side of the satellite is reflective. The attitude control torque along pitch and yaw are quite small as compared with the attitude control torque along yaw axis, especially pronounced at the flip locations (Figure 8). The angles between sunline and velocity vector, as well as sunline and sail normal are observable in Figure 9. The decay in orbit is observable from the semi-major axis given in Figure 10. This is over 35 km decay in one day. This figure is quite significant and may easily realize requirement of de-orbiting within 25 years. On the other hand the eccentricity is slowly increasing, since the solar force is strong at particular locations in orbit. Finally, last plot of Figure 10 shows that the inclination stays the same, since the solar drag force is always in the orbital plane.

Figure 11-14 gives the similar results for Case II, where the inclination is 45 degrees and right ascension of the ascending node is 90 degrees. In this case, pitch and yaw motion of the satellite is observable. The motion is quite smooth, and does not require too much attitude control torque (Figure 12). As similar decay rate in semi-major axis is observable in Figure 14. In the same figure, not only change in orbital eccentricity, but also the change in inclination is observable. In this case, the solar drag force is no longer in the orbital plane, causing a change in the inclination angle. Case III presents the de-orbiting of a polar orbiting satellite. Again both yaw and pitch controls are needed to generate maximum solar drag (Figure 15). The control is smooth, and rather small control torques are needed (Figure 16). The decay rate in semi-major axis is similar to the previous cases. However, the eccentricity does not drift away steadily as it was in the two previous cases. Instead it seems to oscillate periodically. Similarly, the inclination is also oscillating periodically.

CONCLUSIONS

Optimal attitude control to maximize solar drag is mechanized. The mechanization requires only body fixed frame measurements of the sun direction as well as satellite velocity vector direction. The mechanization may be directly used for attitude control, since the to-go quaternion is obtained. Orbit simulations under the effect of maximized solar drag are given for orbits with three separate initial inclinations, while using nonlinear to-go quaternion feedback algorithm. It is shown that, in each case, the maximum solar drag is successfully obtained with the method developed, resulting in similar orbital decays all three cases.

REFERENCES

- ¹ De-orbiting of satellites using solar sails, project proposal, FP7-SPACE-2010-1, 2010.
- ² H. Klinkrad, "Collision risk analysis for low Earth orbit," *Advances in Space Research*, Vol. 13, No. 8, 1993, pp. 177-186.
- ³ N. Johnson, and E.G. Stansbery, "The new NASA orbital debris mitigation procedural requirements and standards," *Acta Astronautica*, Vol. 66, pp. 362-367, 2010.
- ⁴ Anselmo M, Portelli (ASI), Crowther, Tremayne-Smith (BNSC), Alby, Baccini, Bonnal (CNES), Alwes (DLR), Flury, Jehn, Klinkrad (ESA), *European Code of Conduct for Space Debris Mitigation*, Issue 1.0, June 2004.
- ⁵ C.R. McInnes, *Solar sailing technology, dynamics and mission applications*, Berlin: Springer-Praxis, 2004.
- ⁶ B. Wie, *Space Vehicle Dynamics and Control*, AIAA Inc., Reston, VA, 1998.

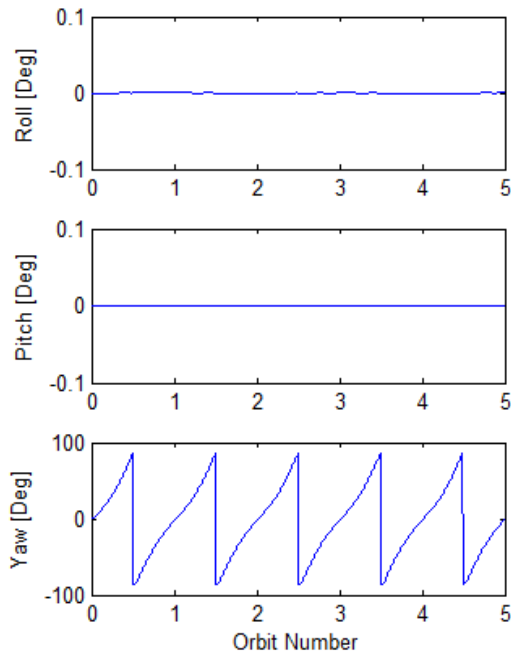


Figure 7 Sail attitude history (Case I)

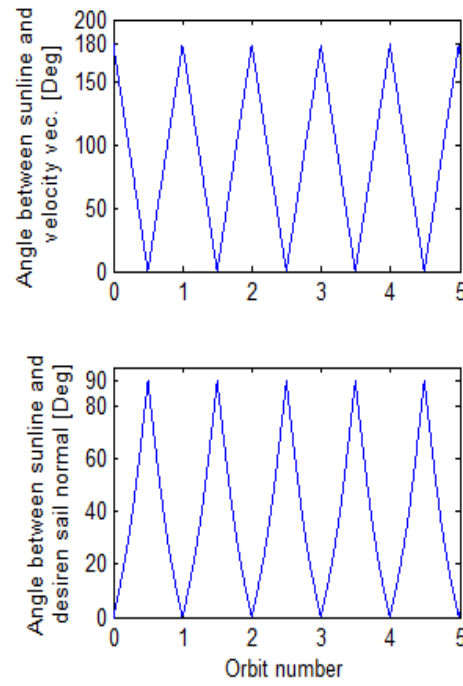


Figure 9 Angle between the sun direction, velocity vector and sail normal (Case I)

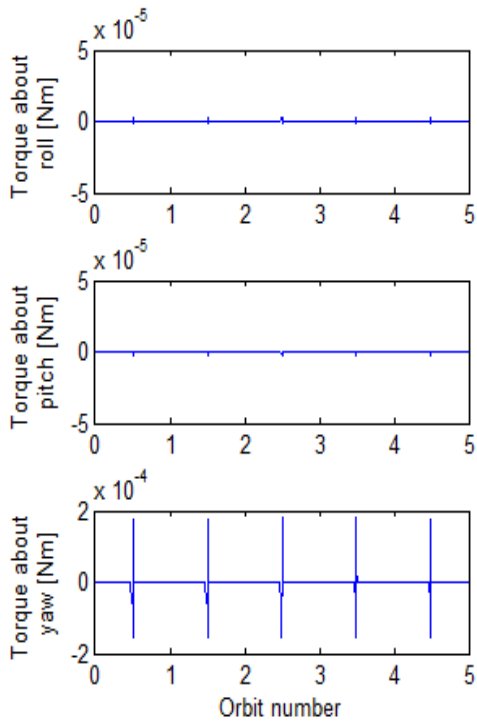


Figure 8 Control torque history (Case I)

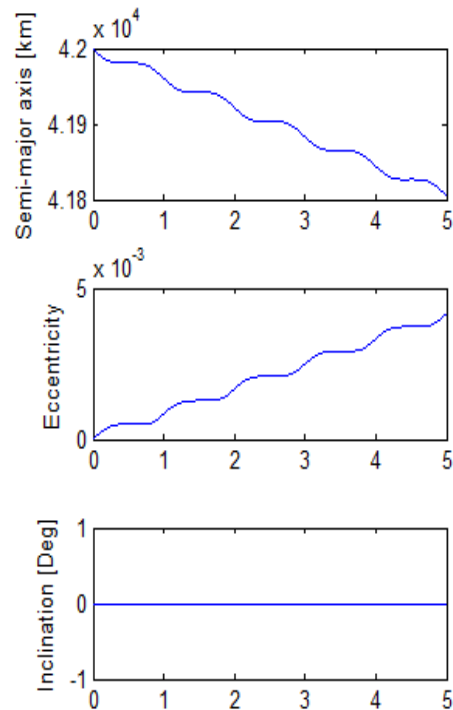


Figure 10 Propagation of orbital elements (Case I)

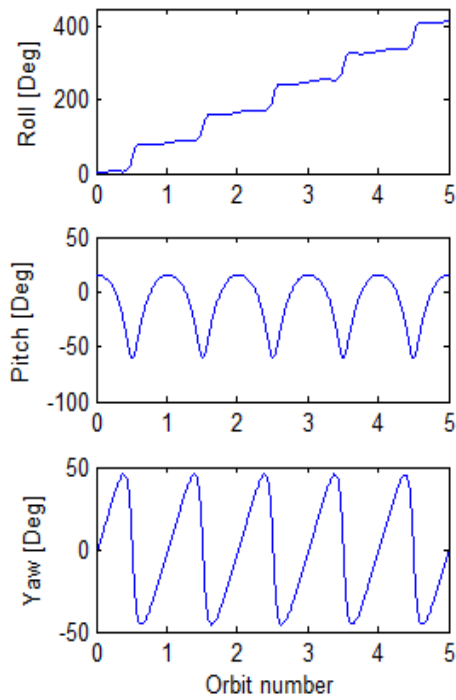


Figure 11 Attitude history (Case II)

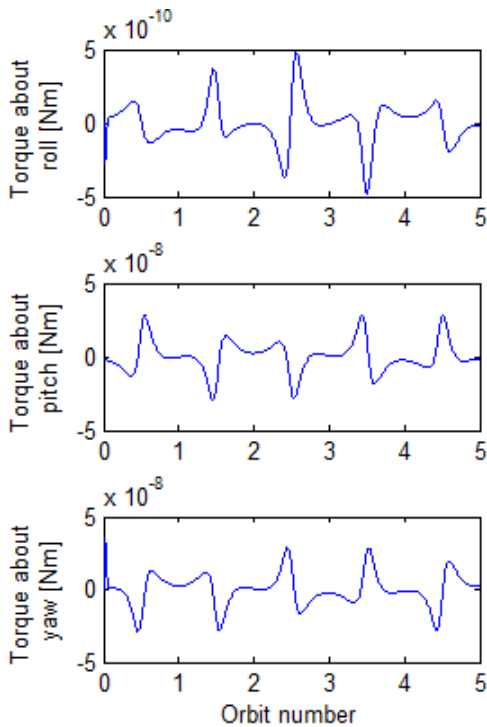


Figure 12 Control torque history (Case II)

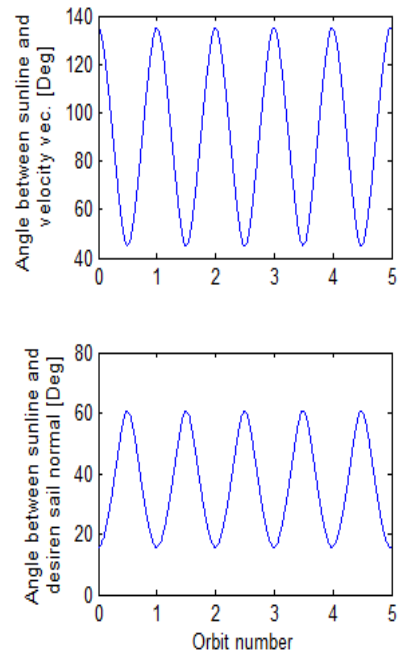


Figure 13 Angles between sun direction, velocity vector and sail normal with (Case II)

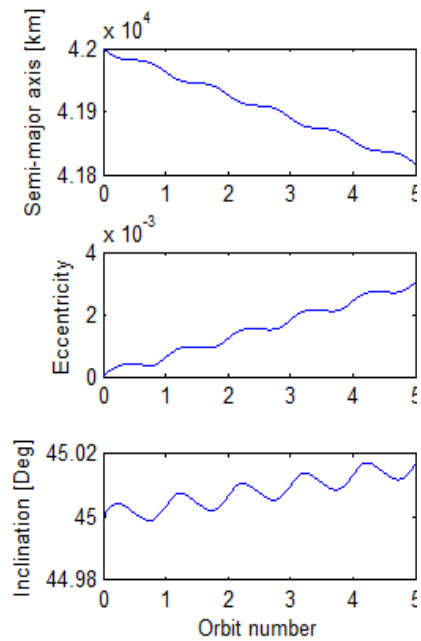


Figure 14 Propagation of orbital elements (Case II)

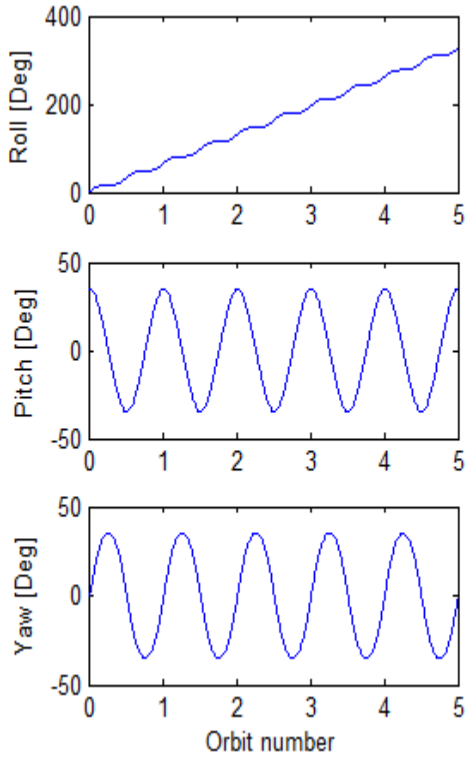


Figure 7 Attitude history (Case III)

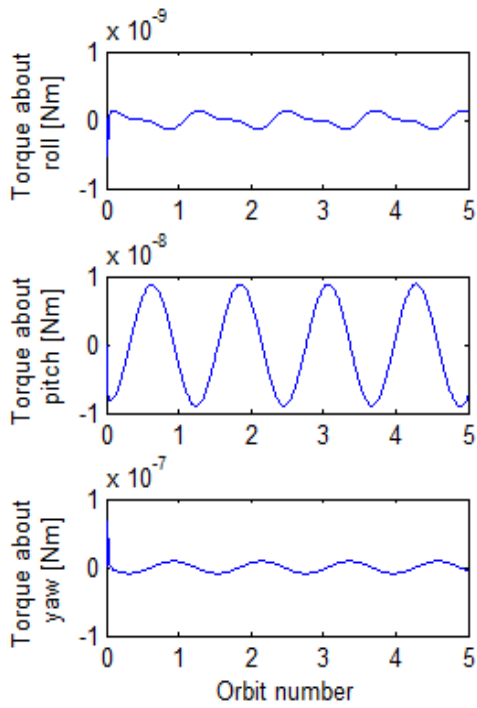


Figure 16 Control torque history (Case III)

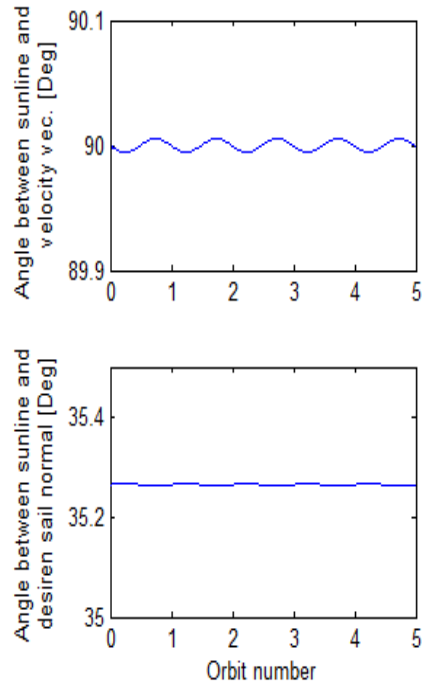


Figure 17 Angles between sun direction velocity vector and sail normal with (Case III)

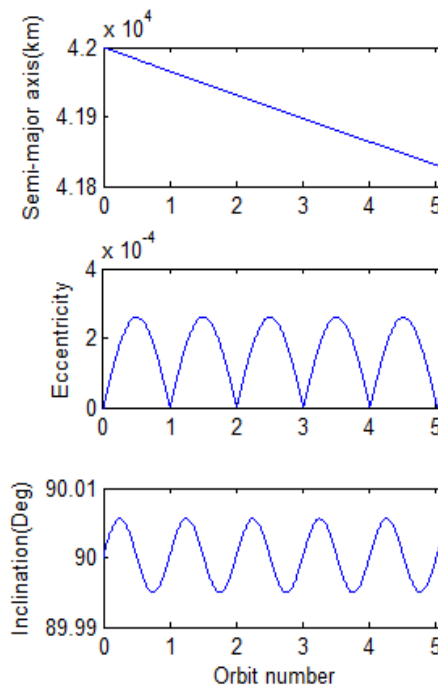


Figure 18 Propagation of orbital elements (Case III)